RED CELL EXTENSIONAL RECOVERY AND THE DETERMINATION OF MEMBRANE VISCOSITY

R. M. HOCHMUTH, P. R. WORTHY, AND E. A. EVANS, *Department of Biomedical Engineering, Duke University, Durham, North Carolina 27706 and Department of Chemical Engineering, Washington University, St. Louis, Missouri 63130 U.S.A.*

ABSTRACT A theory of membrane viscoelasticity developed by Evans and Hochmuth in 1976 is used to analyze the time-dependent recovery of an elongated cell. Before release, the elongated cell is in static equilibrium where external forces are balanced by membrane elastic force resultants. Upon release, the cell recovers its initial shape with a time-dependent exponential behavior characteristic of the viscoelastic solid model. It is shown that the model describes the time-dependent recovery process very well for a time constant in the range of 0.1–0.13 s. The time constant is the ratio membrane surface viscosity η:membrane surface elasticity μ. Measurements for the shear modulus μ of 0.006 dyne/cm give a value for the surface viscosity of red cell membrane as a viscoelastic solid material of $\eta = \mu t_c = (6\text{–}8) \times 10^{-4}$ poise · cm.

INTRODUCTION

Viscoelastic behavior of red cells is observed when the red cell disk is extended (e.g., by pulling at diametrically opposed points on the rim of the cell) and then released. After release, the cell (and its membrane) recovers its original biconcave shape in $\simeq$0.1 s. Because the interior cytoplasm of the red cell is a liquid, the ability to recover its original shape after removing applied forces is the result of elastic energy storage in the membrane (Hochmuth et al., 1973; Evans, 1973; Evans and Hochmuth, 1978). The elastic forces depend only on the amount of deformation and thus can support static loads on the cell. On the other hand, viscous dissipation within the membrane and in the media adjacent to the membrane limit the rate at which the cell recovers its original shape. It can be shown that the loss of mechanical power resulting from dissipation in the cytoplasm and outside aqueous environment is much smaller than the rate of change of elastic energy storage (see Appendix and Evans and Hochmuth, 1976*a*). Therefore, the time rate of recovery is related to the membrane elastic and viscous force resultants.

For displacements on the scale of cellular dimensions and times $>10^{-6}$ s, we can neglect the inertia of the materials involved (see Appendix). The dominant forces that depend on time derivatives of deformation are viscous forces. Consequently, the time-dependent response of membrane deformation to applied forces is limited by the viscous dissipation within the membrane. Dissipative effects in a material are peculiar to the regime of material behavior that is being investigated, i.e., solid, semi-solid, and plastic or liquid (Prager, 1961; Evans and Skalak, 1979). These regimes characterize the material behavior only approximately but they provide an important starting point. The red cell membrane exhibits elastic solidlike behavior for periods of time on the order of 5 min or more (Evans and LaCelle, 1975) provided that

membrane extension ratios are <3–4:1. In other words, the membrane can support static forces at constant deformation without undergoing shear flow. For periods of time in excess of 5–10 min or for membrane extension ratios > ≃3–4:1, the membrane passes through a semi-solid transition to plastic or liquid-like flow (Evans and Hochmuth, 1976*b*). In this paper, we will present data on viscoelastic recovery of elongated red cells and correlate this data with a first order viscoelastic constitutive relation for the red cell membrane. The results will yield an intrinsic time constant for viscoelastic recovery of red cell membrane as a solid material. Also, with the elastic shear modulus data, the coefficient of surface viscosity of the red cell membrane can be determined from the recovery time constant, again for the solid domain of material behavior.

MEMBRANE VISCOELASTIC RECOVERY

The constitutive behavior for a viscoelastic solid may often be quite complicated. However, the first-order formulation simply involves the parallel superposition of two quantities—one that accounts for elastic energy and the other that represents mechanical energy storage loss by viscous dissipation. Such a material that behaves according to this simple supposition principle is called a Kelvin-Voigt solid. The parallel superposition embodies the physical observation that the membrane deformation is both recoverable (memory) and time dependent. The viscoelastic model for a membrane material differs from that for a conventional solid in two ways: (*a*) rheological behavior is described by surface force resultants (tensions) and surface deformation because the membrane is a continuous material only in its surface plane; (*b*) the membrane surface deformation can be large and still recover elastically (Hochmuth et al.,

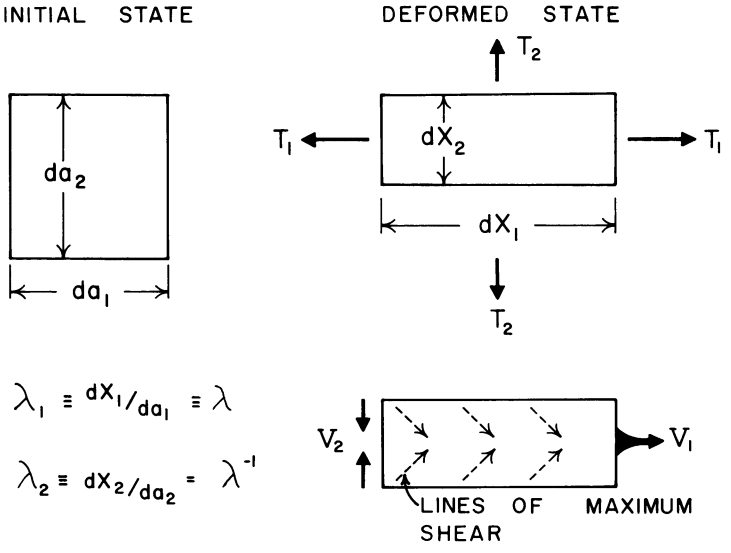

FIGURE 1 Deformation and rate of deformation at constant area of a plane element undergoing a large (finite) extension along one of the principal axes. T_1 and T_2 are principal membrane tensions (force/length). V_1 and V_2 are the principal rates of deformation expressed in terms of the extension ratio λ. The lines of maximum shear occur at $\pm 45°$ to the principal axes.

1973; Evans, 1973). Thus, finite deformation strains (rather than "infinitesimal" or linear strains) are used in the constitutive relation. Fig. 1 illustrates the membrane force resultants (force/unit length) and surface deformation that characterize an element of membrane material. Because the red cell membrane greatly resists area dilation (Evans and Waugh, 1977), the deformations occur at essentially constant element surface area. Thus, only a single extension ratio is required to specify the deformation. The extension ratio, λ, and the principal tension, T_1, are defined by the direction of extension. In this principal direction no shear resultant or shear strain component exists. However, at $\pm 45°$ to the direction of extension, the shear resultant and shear deformation are maximum:

$$T_s = \frac{T_1 - T_2}{2}, \tag{1}$$

$$\epsilon_s = \left(\frac{\lambda^2 - \lambda^{-2}}{4}\right), \tag{2}$$

$$V_s = \frac{V_1 - V_2}{2} = \frac{1}{\lambda}\frac{\partial \lambda}{\partial t}, \tag{3}$$

where T_s is the maximum shear resultant in the membrane (proportional to the difference in principal tensions), ϵ_s is the finite deformation shear strain at constant surface area, V_s is the rate of shear deformation in the membrane surface and t is time. (See Evans and Hochmuth, 1976*a* and 1978; and Evans and Skalak, 1979 for further details.) Elastic constitutive equations involve functional relationships between T_s and ϵ_s. The first-order hyperelastic relation for a membrane is

$$T_s^e = 2\mu\epsilon_s = \frac{\mu}{2}(\lambda^2 - \lambda^{-2}), \tag{4}$$

which has been experimentally verified in detail by Evans (1973), Evans and LaCelle (1975), Waugh (1977), Waugh and Evans (1979), and Brain et al. (1978). The intrinsic material property, μ, is the surface elastic shear modulus. Similarly, nonconservative or viscous constitutive equations involve functional relationships between T_s and V_s. The first-order viscous relation between shear resultant and rate of shear deformation is given by Evans and Hochmuth (1976*a*):

$$T_s^v = 2\eta V_s = \frac{2\eta}{\lambda}\frac{\partial \lambda}{\partial t}, \tag{5}$$

where the coefficient of viscosity for surface shear is η. Eq. 5 describes the material behavior of a "Newtonian" surface liquid.

The first-order constitute equation for a viscoelastic membrane solid is simply the sum of Eqs. 4 and 5,

$$T_s = T_s^e + T_s^v = \frac{\mu}{2}(\lambda^2 - \lambda^{-2}) + \frac{2\eta}{\lambda}\frac{\partial \lambda}{\partial t}. \tag{6}$$

This is the membrane material analogue of the Kelvin-Voigt solid. Eq. 6 can be normalized by

the membrane shear modulus to give a dimensionless form:

$$\frac{T_s}{2\mu} = \frac{1}{4}(\lambda^2 - \lambda^{-2}) + t_c \frac{\partial \ln \lambda}{\partial t}, \tag{7}$$

where $t_c \equiv \eta/\mu$ is the material time constant that characterizes extensional response to force changes in the membrane. Eq. 7 is nonlinear in the extension ratio, λ, because large ("finite") deformations of the membrane are involved.

In any situation where the forces applied to the membrane are zero, the membrane force resultants must also be zero. For such a case, the time-dependent recovery of the membrane extension ratio would be determined by Eq. 7 with the shear resultant equal to zero (Evans and Hochmuth, 1976*a*). The solution is given in terms of the extension ratio, λ_m, which occurs at the instant when the forces are set to zero:

$$\lambda(t) = \left[\frac{\Lambda + e^{-t/t_c}}{\Lambda - e^{-t/t_c}}\right]^{1/2}, \tag{8}$$

where

$$\Lambda \equiv \frac{\lambda_m^2 + 1}{\lambda_m^2 - 1}.$$

For small deformations ($\lambda \to 1$), Eq. 8 reduces to the exponential recovery relation for a linear viscoelastic solid.

In the Appendix, we demonstrate that the mechanical power loss resulting from viscous drag on the membrane by the cytoplasm and extracellular fluid is much smaller than the mechanical power produced by membrane elastic forces when the recovery time is greater than a few milliseconds. Thus, after the elongated red cell is released, the elastic energy stored in the membrane is dissipated by viscous mechanisms within the membrane. The net membrane force resultants are zero and the extensional recovery of each membrane material element can be modeled to first order by the viscoelastic recovery (Eq. 8).

EXTENSIONAL RECOVERY OF HUMAN RED BLOOD CELLS

The purpose of this study is to use Eq. 8 to measure the time constant, t_c. This is accomplished by measuring the rate at which a red cell disk recovers its biconcave shape after the removal of an external force of deformation applied at equal and opposite points on the red cell rim. Because accurate values for the surface elastic constant, μ, have been determined ($\pm 15\%$, e.g., Waugh, 1977; Waugh and Evans, 1979; and Brain et al, 1978), a measurement for t_c ($t_c = \eta/\mu$) permits the calculation of the surface viscosity, η, in the solid material domain. This provides an assessment of the surface viscosity of a biological membrane at the macroscopic (i.e., continuum) level.

In the recovery of elongated red cells, we observe the extrinsic geometry of the cell as a function of time. We measure the overall length and width of the plane image of the cell. However, the intrinsic deformation at local points in the membrane is not uniform. The time dependence of the local deformation in the membrane will follow the viscoelastic recovery at the material point because the forces from the adjacent fluids can be neglected (see Appendix). Consequently, we can describe the evolution of the material deformation over the

cell membrane envelope by the following equation:

$$\lambda(\mathbf{x}, t) = \left[\frac{\Lambda(\mathbf{x}) + e^{-\bar{t}}}{\Lambda(\mathbf{x}) - e^{-\bar{t}}}\right]^{1/2}, \tag{9}$$

where $\bar{t} \equiv t/t_c = \mu t/\eta$ and

$$\Lambda(\mathbf{x}) \equiv \frac{\lambda_m^2(\mathbf{x}) + 1}{\lambda_m^2(\mathbf{x}) - 1}.$$

Here, the deformation, λ, throughout the membrane surface is a function of the position, $\mathbf{x}$, on the membrane. If Eq. 9 were linear, we could simply integrate over the cell surface (from one end to the other) to determine the instantaneous length and width of the cell.

The red cell experiment involves extension and subsequent recovery of the whole red blood cell that is pulled at diametrically opposed positions on the equatorial rim. Fig. 2 is a time sequence of photographs that show a cell returning to its undeformed shape. During the extension and recovery process the extension ratio is nonuniform over the membrane surface and is difficult to determine analytically because it involves the solution of nonlinear equations of membrane equilibrium over the entire membrane surface. However, most of the upper and lower surfaces of the red cell membrane are essentially shaped like flat disks with only axial tension along the direction of extension. Thus, it is possible to investigate the effects of the nonuniform extension in the plane of the disk (Evans and Skalak, 1979). This approach was used by Evans (1973) to investigate the elastic behavior of fluid shear deformed red cells that form point attachments to glass. With this approach, the numerical procedure is to cut the disk into finite strips normal to the axis of extension. The initial dimensions of the strips are determined by force equilibrium and constant area deformation. The initial force equilibrium states that the axial force must be constant throughout the disk along the direction of extension. The local extension ratio is then related to the axial force with the elastic

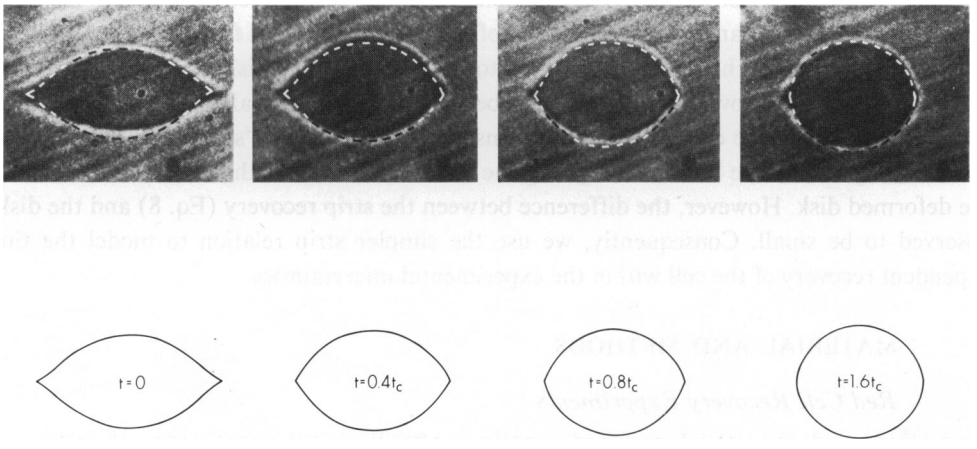

FIGURE 2 Comparison of the recovery of a membrane disk with a red blood cell. In this particular case, the time constant t_c for the red blood cell is 0.10 s. Note at maximum extension that the width of the cell is slightly less than that of the flat disk, indicating that the cell is "rounding-up" to some extent. Note also the slight asymmetry in the red cell.

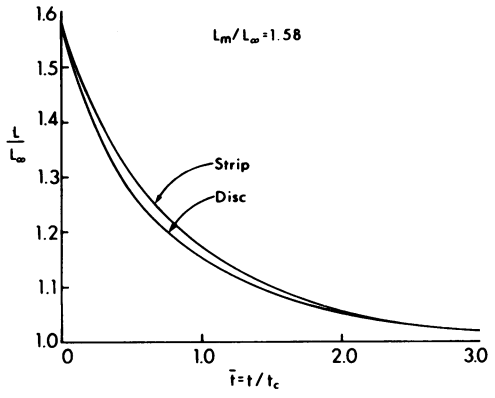

FIGURE 3

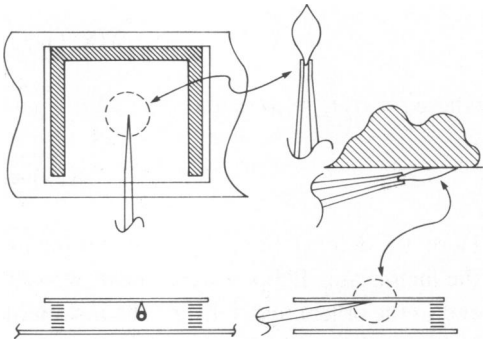

FIGURE 4

FIGURE 3 Comparison of the recovery curve for a membrane strip with that for a membrane disk initially deformed by pulling at diametrically opposite points. L is the overall length of the disk or strip at any time t. L_m and L_∞ are the initial (maximum) and final lengths of the disk or strip. The time constant t_c is the ratio of membrane surface viscosity η to membrane surface elasticity μ: $t_c \equiv \eta/\mu$.

FIGURE 4 Schematic of the chamber in which red cells are deformed. Cells that adhere to both the top surface (shown) and the bottom surface are deformed by gently aspirating a portion of the rim into a micropipette and then slowly withdrawing the micropipette until the cell is released. After release, the cell recovers its undeformed shape as shown in Fig. 2.

constitutive relation (Eq. 4). (Note that the axial tension, T_1, is twice the shear resultant T_s [Eq. 1] and that the local axial tension multipled by the local width of the strip is equal to the axial force. The force resultants in the direction normal to extension are assumed to be small because buckling or "rounding-up" of the cell is not observed for the extensions applied to the cell.) The end elements of the disk at the attachment points are integrable singularities as analyzed by Evans (1973) and are represented by triangular elements of appropriate dimensions in the deformed state. The extension ratio increases rapidly close to the attachment location; consequently, the regions proximal to the locations where the cell is pulled recover faster than the central portion of the cell, as is evident from Eq. 8 or 9. The line drawings in Fig. 2 are the computer solution to the extension and disk recovery as prescribed by Eq. 9; the rapid recovery of the ends can be seen here. The overall length of the disk also recovers faster than the case of uniform extension of a membrane "strip"; the comparison is shown in Fig. 3 with the lower curve giving the time dependence of the end-to-end distance of the deformed disk. However, the difference between the strip recovery (Eq. 8) and the disk is observed to be small. Consequently, we use the simpler strip relation to model the time-dependent recovery of the cell within the experimental uncertainties.

MATERIAL AND METHODS

Red Cell Recovery Experiments

Fresh blood was drawn into a heparinized vacutainer. After the initial centrifugation, the plasma and buffy coat was removed by aspiration. The cells were washed once in phosphate-buffered saline (PBS; 6.375 g NaCl; 3.143 g Na_2HPO_4; 0.738 g KH_2PO_4; 2.0 g penicillin-G, catalog No. PEN NA, Sigma Chemical Co., St. Louis, Mo.) and resuspended at a volume concentration of 0.05% in the same PBS solution as above plus 0.1% by weight of bovine serum albumin (BSA), and 0.1% by weight glucose. The

red cell suspension was injected into a reservoir (Fig. 4) made of two cover slips and a parafilm gasket. The bottom surface was a 24 × 60-mm No. 1 cover slip, and the top surface was a 22 × 30-mm No. 1 cover slip. The walls were formed by several thicknesses of Parafilm (American Can Co., Marathon Products, Neenah, Wisc.) cut in the shape of a block "U." The cells were allowed to settle and subsequently attach to the lower or upper surface for 20 min, and then a native plasma solution (centrifuged at 19,000 rpm for 15 min to remove platelets and then diluted 1:10 with PBS) was gently injected into the reservoir to displace two reservoir volumes. This prevented additional cell attachment.

Cell deformation was produced by aspirating a small portion of the rim of the red cell into the tip of a micropipette and gently withdrawing the micropipette (Fig. 4); then, the rim of the cell was released and the cell returned to its original biconcave shape (Fig. 2). The pipette extension of the cell took only a few seconds and the recovery tenths of a second. The pipettes (11-10-L, Frederick Haer and Co., Brunswick, Mass.) had a nominal 0.5-μm i.d. The working diameter of $\simeq$0.7–1.0 μm was obtained by breaking the end of the pipettes against the square edge of a microslide. This created a square-edged tip. The micropipettes were filled with the same PBS solution that the cells were washed with. The aspiration pressure was achieved by lowering a water-filled reservoir (which was open to atmosphere and attached to the pipette by Tygon tubing, U.S. Stoneware Co., Akron, Ohio) below the level of the microscope stage. The micropipette was mounted in a de Fonbrune micromanipulator (Orion Research Inc., Cambridge, Mass.).

Red cell recovery was observed with a Zeiss inverted microscope (Carl Zeiss, Inc., New York) with Zeiss bright field optics (63X, 1.25 N.A. Neofluor oil immersion objective and a 1.4 N.A. oil immersion condensor). The recovery process was recorded on either video tape or 16 mm film. In the first case, a Panasonic camera (WV241P, Panasonic Co., Franklin Park, Ill.) and a Javelin X-400 stop action video tape recorder (Javelin Division of Apollo Lasers, Los Angeles, Calif.) with a 0.01 s video timer (G-77 time-date generator, Odetics, Inc., Anaheim, Calif.) was used. The video scanning rate was 60/s, producing a "data point" every 16.7 ms. Cell length was measured with a Vector Calculator (Vista Electronics, La Mesa, Calif.) that imposed two (manually) movable cursors on the video screen and displayed a number proportional to the distance between the two cursors.

When necessary for better image and time resolution, 16 mm Tri X reversal film and a high-speed camera (Hycam; 400 ft., Red Lake Laboratories, Santa Clara, Calif.) at nominal framing rates between 100 and 200/s were used to record the recovery process. Time was marked at the edge of the film with light "dots" flashed at a rate of 100/s. Exposure times with the 1/2.5 shutter were between 1/250 and 1/500 s. The developed film was displayed on white paper with an L & W stop action projector (Red Lake Laboratories). Measurements were made directly, one at a time. At 200 frames/s, a data point is produced every 5 ms.

RESULTS AND DATA CORRELATION

Typical changes in length of a cell with time during the recovery process are shown in Figs. 5 and 6. In Fig. 5, cell recovery was recorded on 16 mm film at 185 frames/s (5.4 ms/frame),

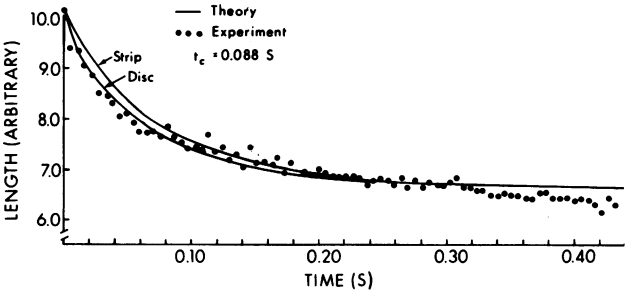

FIGURE 5 Viscoelastic recovery of a red cell compared to that of a membrane strip and disk where the resting length of the strip and disk is set equal to the cell length at 0.3 s (three time constants).

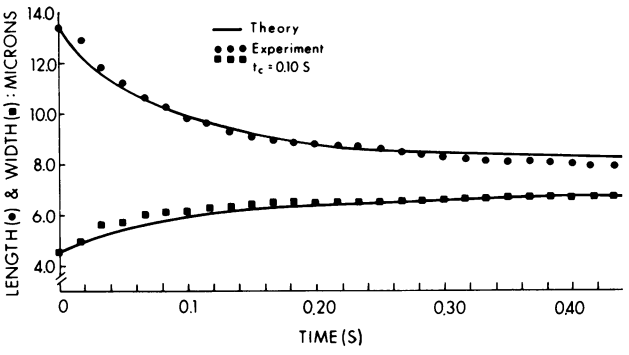

FIGURE 6 Viscoelastic recovery of overall cell length and maximum cell width. The simultaneous length and width measurement are made on the same cell. The time constant t_c is calculated from the length data and then applied to the width data.

whereas in Fig. 6 cell recovery was recorded on video tape at 60 pictures/s. Fig. 6 shows, also, the change in width of a single cell during the recovery process. In all experiments the initial cell length was taken as the length of the cell at that instant when the rim is just free from the micropipette. However, the final length of the cell is not easily identified because the projections formed at the attachment locations recover only after several seconds have elapsed. To obtain the first results of this section, the length of the cell at 0.3 s (approximately three time constants) was arbitrarily picked as the resting length, and the least squares fit of Eq. 8 to the data over the range of $0 \leq t \leq 0.4$ s was determined by computer for an optimum value of the time constant, t_c.

Fig. 5 illustrates the results for a single cell recovery; the upper curve is Eq. 8 for $t_c = 0.088$ s and $\lambda_m = 1.54$. The data for less than one time constant appear to recover somewhat faster than the theoretical curve for a strip. However, the results for the disk (lower curve in Fig. 5) closely match the experimental results for the entire range, $t \leq 0.3$ s. In addition, the disk analysis provides the comparison of theory and experiment shown in Fig. 2. Note, however, at $t = 0$, that the minor axis of the deformed red cell in Fig. 2 is slightly less than that of the deformed disk; this is the result of the curved membrane contour. The width recovery data is shown as the lower curve in Fig. 6, along with the corresponding length data for the same cell. For the width recovery, the extension ratio is given by the inverse relation, $\lambda = W_\infty / W$, which also correlates with Eq. 8. Using this approach, 46 initial recovery experiments were performed at room temperature, with 28 being recorded on video tape and 18 on high-speed

TABLE I
VALUES FOR THE TIME CONSTANT AT ROOM TEMPERATURE (25°C), DETERMINED FROM CELL LENGTH RECOVERY MEASUREMENTS

	Mean ± SE	Pulls	Cells	Donors
	s			
Inclined slide, top surface (Fig. 4)	0.096 ± 0.013	19	4	2
Level slide, bottom surface	0.101 ± 0.013	27	8	3
Overall	0.099 ± 0.013	46	12	4

film. The results are identical in either case with cells attached to the upper glass surface in some cases and with cells attached to the lower glass surface in the other cases (Table I).

It is apparent in Fig. 2 that the major portion of the cell membrane recovers with an exponential-like behavior that is well modeled by Eq. 9. However, the membrane material at the attachment locations shows a much slower recovery phase at long time periods (after several t_c). Thus, an absolute measure of the length is compromised by this small uncertainty. At the attachment points, such large extension ratios exist that the rheological equation is inappropriate; indeed plastic flow of a small microfilament of membrane eventually occurs at the glass attachment location (Hochmuth et al., 1973; Evans and Hochmuth, 1976*b*). Because the attachment locations represent less than a few percent of the cell membrane area, we developed a procedure designed to eliminate the effect on absolute length dimension. This approach is suggested by the results in Fig. 6 for length and width data that recover in a complementary manner. For a simple membrane material element or strip, the length divided by the width is the extension ratio squared, which is dimensionless. Here, the viscoelastic recovery is simply

$$\frac{L}{W} = \left(\frac{L}{W}\right)_\infty \cdot \frac{\Lambda + e^{-\bar{t}}}{\Lambda - e^{-\bar{t}}}, \tag{10}$$

where

$$\Lambda \equiv \frac{\left(\frac{L}{W}\right)_m + \left(\frac{L}{W}\right)_\infty}{\left(\frac{L}{W}\right)_m - \left(\frac{L}{W}\right)_\infty}.$$

The length (L):width (W) ratio is subscripted by $(\ )_m$ for initial values and $(\ )_\infty$ for long times. The L:W ratio does not have to approach unity. With Eq. 10, the least squares fit to the L:W ratio vs. time is found for optimum values of time constant, t_c, and final aspect ratio, $(L/W)_\infty$. Typical experimental results are shown in Fig. 7. To fit Eq. 10 to the data shown in Fig. 7, the values for the two parameters, $(L/W)_\infty$ and t_c, are chosen to minimize the sum of the squares of the errors between the viscoelastic model (Eq. 10) and experimental values for L/W. Thus, for N data points the following functional is minimized by choosing optimum values for $(L/W)_\infty$ and t_c:

$$\epsilon^2 = \sum_1^N \left[\left(\frac{L}{W}\right)_{\text{expr}} - \left(\frac{L}{W}\right)_{\text{theo}}\right]^2 \Big/ N,$$

where ϵ is the root mean square error per datum point. For the four sets of results shown in Fig. 7, the values for ϵ range from 0.013 to 0.020. This error corresponds to errors in length and width measurements of $\cong$0.1 μm. Thus, the errors are within the limits of optical resolution of the measuring system.

The rearrangement of Eq. 10, *viz.*,

$$\frac{\left(\frac{L}{W}\right) - \left(\frac{L}{W}\right)_\infty}{\left(\frac{L}{W}\right) + \left(\frac{L}{W}\right)_\infty} \cdot \frac{\left(\frac{L}{W}\right)_m + \left(\frac{L}{W}\right)_\infty}{\left(\frac{L}{W}\right)_m - \left(\frac{L}{W}\right)_\infty} = e^{-t/t_c} \tag{11}$$

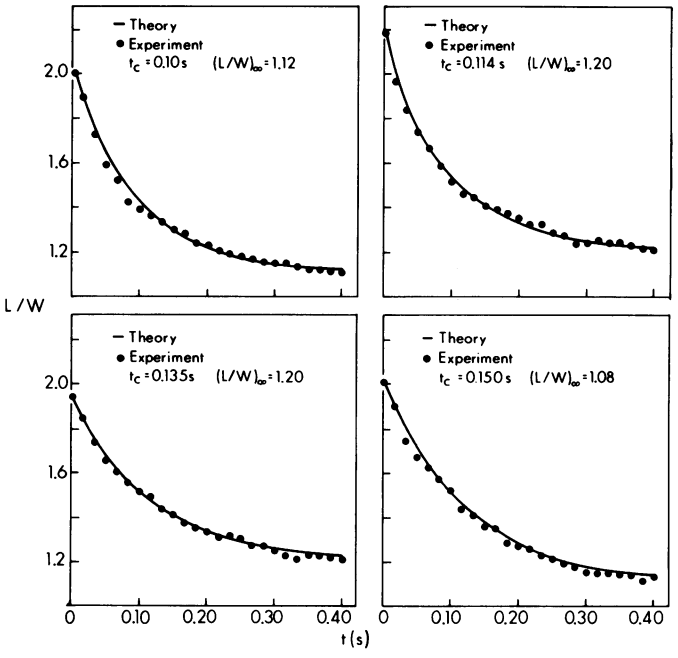

FIGURE 7 Cell recovery data in terms of the L:W ratio for four different cells. The values of t_c and $(L/W)_\infty$ for the theoretical curve (Eq. 10) are chosen to give a least-squares fit to the data.

shows that data from different experiments can be "collapsed" onto a single exponentially decaying curve as shown in Fig. 8 for the four sets of results from Fig. 7. Although not shown, the experimental results for $\bar{t} > 4.0$ fall on the horizontal axis plus or minus the typical error per point ϵ (± 0.02).

For the 16 experiments to date that have been analyzed in terms of the L:W ratio, the time constant is determined to be $\simeq$20% greater than that based simply on length recovery data, i.e., $t_c = 0.123 \pm 0.020$ s. Thus, the method of data analysis and correlation does not significantly affect the time constant that is obtained. As is observed in Fig. 5–8, the viscoelastic model correlates well with the observed cell recovery.

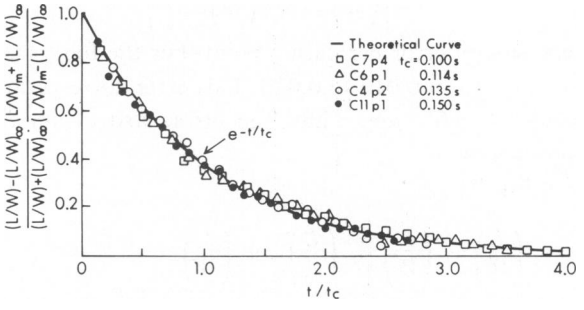

FIGURE 8 Data from Fig. 7 replotted according to Eq. 11.

DISCUSSION

From the analysis in the Appendix, it appears that neither inertial forces nor external viscous forces will interfere with the recovery process. This, along with the results presented in Figs. 5–8, indicates that the time-dependent recovery process is adequately modeled by the Kelvin superposition principle (Eqs. 8 and 10) with the elastic and viscous constitutive components given by Eqs. 4 and 5.The nonuniform distribution of extension has little effect on the predicted time dependence of the cell shape recovery; also, the simple disk extension model correlates well with the projected cell images. If the attachment point effects are excluded, error analysis indicates that the distribution in data about the time-dependent recovery curve is within the limits of optical resolution.

The linearization of the viscoelastic model (Eq. 8) results in the classical Kelvin-Voigt model in which a linear elastic spring and viscous dashpot are in parallel. Thus, the linearized version of Eq. 11 is

$$\frac{\left(\frac{L}{W}\right) - \left(\frac{L}{W}\right)_\infty}{\left(\frac{L}{W}\right)_m - \left(\frac{L}{W}\right)_\infty} = e^{-t/t_c}.$$

This equation also provides a good fit for the data shown in Figs. 7 and 8 except for the first few data points (excluding $t = 0$) where the value for L/W is on the order of 2:1 and, therefore, higher order (nonlinear) terms cannot be neglected.

Our finite deformation viscoelastic model is especially useful when extension ratios are quite large as in the recent interesting experiments of Sung and Chien (1978). In these experiments, Sung and Chien aspirated a portion of the red cell membrane into a pipette (Evans, 1973) and then studied the time-dependent recovery within the pipette of the aspirated portion upon removal of the suction pressure. The analysis of the experiment of Chien et al. (1978) with the viscoelastic model (Evans and Hochmuth, 1976*a*) for over 100 red cells gives a value for the recovery time constant of 0.13 ± 0.05 s, which agrees with the data presented in this study. Because the results obtained by the two different mechanical experiments give essentially the same result, we conclude that the recovery time constant is an intrinsic property of the red cell membrane material, independent of the cell geometry and external dissipation. In addition, the experimental observation shows that the viscoelastic constitutive relation models the recovery process for the large range of material extension involved during the recovery phase and, therefore, we can determine the coefficient for membrane surface viscosity in this solid material domain.

Clearly, the red cell membrane is a heterogeneous and complicated material capable of different types of material behavior. For the range of forces (membrane shear resultants) and times in the present experiments the membrane behaves as a viscoelastic solid. Within the limitations of microforce experiments on cells, the recovery behavior of the membrane is adequately described by a Kelvin-Voigt superposition. However, the membrane can exhibit other types of material behavior. For example, for relatively large shear resultants (or extension ratios) Hochmuth et al. (1973) have shown that the membrane will yield and deform plastically (i.e., permanently). We have modeled this plastic flow behavior by assuming that the membrane behaves as a two-dimensional Bingham plastic (Evans and

Hochmuth, 1976*b*). In addition, "moderate" membrane deformations (below the plastic yield point) that are imposed for long periods of time (on the order of 10 min) result in membrane "creep" (Evans and LaCelle, 1975). A material that creeps is often called a viscoelastic fluid. In this case a "Maxwell model," which consists of elastic and viscous terms in series (so that the sum of the finite deformation of the individual elastic and viscous components would equal the total deformation of the membrane), would be used to model the deformation process (Evans and Skalak, 1979).

The viscoelastic model described in the present paper is specific to the domain of solid material behavior. Longer times or larger forces result in semi-solid relaxation behavior (creep) and plastic flow, respectively. In the solid material domain, our experiments and those of Sung and Chien (1978) can be used to determine a value for the membrane surface viscosity. Thus, because $\mu \approx 0.006$ dyne/cm (25°C) (Waugh, 1977; Waugh and Evans, 1979; Brain et al., 1978) and $t_c \approx 0.10$–0.13 s, then $\eta = \mu t_c = (6 - 8) \times 10^{-4}$ poise · cm.

We thank Steve Cannon, David Markle, and S. T. Smith for programming the computer to reduce the data and David Markle for the computer solution to the disk recovery problem. Karen Buxbaum obtained the data shown in Fig. 6.

Both R.M.H. and E.A.E. are supported by National Institutes of Health Research Career Development Awards, HL 70612 and HL 00063. In addition, this work was supported by National Institutes of Health grant HL 21803 (R.M.H.), HL 12839 (P.R.W.), and HL 16711 (E.A.E.).

Received for publication 17 December 1977 and in revised form 18 November 1978.

REFERENCES

BRAIN, M. C., I. KOHN, A. J. MCCOMAS, Y. F. MISSIRLIS, M. P. RATHBONE, and J. VICKERS. 1978. Red-cell stability in Duchenne's syndrome. *N. Engl. J. Med.* **298**:403.

CHIEN, S., K.-L. P. SUNG, R. SKALAK, S. USAMI, and A. TOZEREN. 1978. Theoretical and experimental studies on viscoelastic properties of red cell membrane. *Biophys. J.* **24**:463.

EVANS, E. A. 1973. New membrane concept applied to the analysis of fluid shear- and micropipette-deformed red blood cells. *Biophys. J.* **13**:941.

EVANS, E. A., and R. M. HOCHMUTH. 1976*a*. Membrane viscoelasticity. *Biophys. J.* **16**:1.

EVANS, E. A., and R. M. HOCHMUTH. 1976*b*. Membrane viscoplastic flow. *Biophys. J.* **16**:13.

EVANS, E. A., and R. M. HOCHMUTH. 1978. Mechanochemical properties of membranes. *In* Current Topics in Membranes and Transport. F. Bronner and A. Kleinzeller, editors. Academic Press, Inc. **10**:1.

EVANS, E. A., and P. L. LACELLE. 1975. Intrinsic material properties of the erythrocyte membrane indicated by mechanical analysis of deformation. *Blood.* **45**:29.

EVANS, E. A., and R. SKALAK. 1979. Mechanics and Thermodynamics of Biomembranes. CRC Press, West Palm Beach, Florida. In press.

EVANS, E. A., and R. WAUGH. 1977. Osmotic correction to elastic area compressibility measurements on red cell membrane. *Biophys. J.* **20**:307.

HOCHMUTH, R. M., N. MOHANDAS, and P. L. BLACKSHEAR, JR. 1973. Measurement of the elastic modulus for red cell membrane using a fluid mechanical technique. *Biophys. J.* **13**:747.

PRAGER, W. 1961. Introduction to Mechanics of Continua. Dover, New York.

SUNG, P. K. L., and S. CHIEN. 1978. Viscous and elastic properties of human red cell membrane. Presented at The 70th Annual American Institute of Chemical Engineers Meeting, 18 November 1977. American Institute of Chemical Engineers Symposium Series. **71**:81.

WAUGH, R. E. 1977. Temperature dependence of the elastic properties of red blood cell membrane. Ph.D. thesis. Duke University.

WAUGH, R. E., and E. A. EVANS. 1979. Thermoelasticity of red blood cell membranes. *Biophys. J.* **26**:115.

APPENDIX

The purpose of this appendix is to show that the rate of dissipation in the bulk hemoglobin phase is small compared to that in the plane of the membrane; thus, dissipation in the hemoglobin solution does not retard the recovery process. In addition it is shown that the inertial forces experienced by both membrane and hemoglobin solution during the recovery process are extremely small when compared to the viscous forces.

Dissipation in Cytoplasm and Membrane

During the recovery process, the rate of dissipation in the hemoglobin solution contained inside the cell is simply the rate at which work is done on the boundary of the system (i.e., the membrane). The rate of doing work is the mechanical power, $\dot{W}$. For a local region of a Newtonian fluid (e.g., the hemoglobin or extracellular solutions), the mechanical power per unit volume is given by the medium viscosity times the square of the local rate of shear deformation. In the red cell extension and recovery experiments, it is observed that the projected cell area, A_c, remains essentially constant throughout the experiment. Because the interior volume is constant, the mean cell thickness, δ, is essentially constant during the experiment. Consequently, fluid layers between the upper and lower cell surfaces experience deformation that is geometrically similar to the cell projection. Therefore, the rate of shear deformation in the cell interior is approximately the same as the rate of shear deformation, V_s, in the membrane surface. With this approximation, we estimate the mechanical power dissipated inside the cell to be on the order of

$$\dot{W}_{\text{Hb}} \sim \eta_{\text{Hb}} \cdot V_s^2(A_c \cdot \delta), \tag{A1}$$

where $\tilde{\eta}_{\text{Hb}}$ is the viscosity (poise) of the hemoglobin solution. The mechanical power that is dissipated in the membrane is estimated by a similar relation for the upper and lower disk surfaces,

$$\dot{W}_m \sim \eta V_s^2(2A_c), \tag{A2}$$

where η is the surface viscosity (poise-cm) of the membrane. For a viscoelastic solid that is represented by the parallel addition of elastic and viscous processes, the coefficient of viscosity can be replaced by the recovery time constant times the elastic shear modulus; therefore, Eq. A2 becomes

$$\dot{W}_m \sim (t \cdot \mu) V_s^2(2A_c). \tag{A3}$$

The ratio of mechanical power dissipated in the cytoplasm to that dissipated in the cell membrane is given by the quotient of Eqs. A1 and A3,

$$\frac{\dot{W}_{\text{Hb}}}{\dot{W}_m} \sim \frac{\tilde{\eta}_{\text{Hb}} \cdot \delta}{2(t \cdot \mu)}. \tag{A4}$$

The hemoglobin solution viscosity is on the order of 10^{-1} poise; the elastic shear modulus is 6×10^{-3} dyne/cm; and the cell thickness is on the order of 2×10^{-4} cm. Therefore, the ratio is inversely proportional to the measured recovery time,

$$\frac{\dot{W}_{\text{Hb}}}{W_m} \sim \frac{10^{-3}}{t}.$$

Thus, for time constants greater than a millisecond, membrane dissipation exceeds the dissipation in the hemoglobin solution. Because the extensional recovery time constant was measured to be 10^{-1} s, the dissipation in the hemoglobin solution inside the cell is negligible compared to the membrane dissipation.

In the discussion given above, we have shown that dissipative effects within the internal cytoplasm can be neglected in comparison to that in the membrane. In addition, the extracellular fluid appears to have

no effect on the recovery process because the viscosity of the extracellular fluid is $\simeq 1/10$ that of hemoglobin. Also, if the extracellular fluid retarded the recovery process, then the cell shape would be asymmetric (teardrop shape) during the recovery phase. Also, the time of recovery would be greatly influenced by the distance of the cell membrane from the nearby surface. The results in Table I indicate that the proximity of the glass surface does not affect the results.

Inertial Effects

The "Reynolds number," Re, provides a measure of the ratio of inertial (momentum) forces to viscous forces. Small values for the Reynolds number indicate that momentum effects are not important and lead to what is often called "Stokes flow" or "creeping flow." Because the Reynolds number is directly proportional to some characteristic distance or displacement, deformation processes at the cellular level are almost always at very low Reynolds numbers. For the characteristics velocities (e.g., 1 μm in 0.1 s or 10^{-3} cm/s), densities (10^{-6} g/cm^2 for membrane and 1 g/cm^3 for hemoglobin), distances (10^{-4} cm) and viscosities (10^{-3} poise-cm for membrane and 10^{-1} poise for hemoglobin) in these experiments, the Reynolds numbers are

$$\mathrm{Re}_{\mathrm{Hb}} = \frac{\rho VD}{\mu} = \frac{1 \times 10^{-3} \times 10^{-4}}{10^{-1}} = 10^{-6}$$

and

$$\mathrm{Re}_m = \frac{10^{-6} \times 10^{-3} \times 10^{-4}}{10^{-3}} = 10^{-10}.$$

Clearly, inertial forces play no role in the recovery process.